The First Phenalenyl-Based Neutral Radical Molecular Conductor

X. Chi,[†] M. E. Itkis,[†] B. O. Patrick,[†] T. M. Barclay,[‡] R. W. Reed,[§] R. T. Oakley,[§] A. W. Cordes,[‡] and R. C. Haddon*,[†]

Contribution from the Departments of Chemistry and Physics, Advanced Carbon Materials Center, University of Kentucky, Lexington, Kentucky 40506-0055, Department of Chemistry and Biochemistry, University of Arkansas, Fayetteville, Arkansas 72701, and Department of Chemistry, University of Waterloo, Waterloo, Ontario N2L 3G1, Canada

Received June 16, 1999

Abstract: We report the preparation, crystallization, and solid-state characterization of a spiro-biphenalenyl radical. The crystal structure shows that the radical is monomeric in the solid state and without intermolecular contacts that fall within the van der Waals atomic separation. Magnetic susceptibility measurements show Curie behavior (1 spin per molecule) throughout the temperature range 10−400 K, confirming the presence of noninteracting spins in the solid. The compound shows a room-temperature conductivity of $\sigma = 0.05$ S/cm, the highest yet for a neutral radical conductor. We suggest that the ground state of the radical corresponds to a degenerate Mott−Hubbard insulator. We postulate the presence of delocalized energy bands that are responsible for the transport properties but that are separated from the insulating ground state by an energy gap corresponding to the on-site Coulombic correlation energy. Given the presence of isolated molecules in the crystal lattice, the magnitude of the conductivity, the finding of band transport, and the width of the conduction band (0.5 eV) are unprecedented.

Introduction

New classes of conductors usually rely on charge-transfer for the introduction of the optimum number of charge carriers. The cuprate and C_{60} superconductors are cases in point. For some time we have attempted to prepare an intrinsic molecular metal, that is, a solid composed of a single molecular species that would function as a classical (mono)atomic metal and superconductor.[1,2] This necessarily requires the crystallization of a neutral radical, and we have argued in favor of the phenalenyl system. While some interesting derivatives have been prepared,[3,4] it has not been possible to crystallize any of the likely candidates (although Nakasuji has reported a sterically hindered system that exists as a π-dimer).[5] To date, the only progress in the field of neutral radical conductors has come through the sulfur−nitrogen compounds reported by Oakley and co-workers.[6,7]

There are a number of difficulties in the realization of a molecular metal based on phenalenyl: (1) The strength of the carbon−carbon bond makes it difficult to suppress σ-dimerization. (2) Like most delocalized organic radicals, phenalenyl is planar and therefore predisposed to the formation of one-dimensional stacks which are subject to electronic instabilities with insulating ground states. (3) Radicals are usually expected to give rise to exactly half-filled bands, which are especially prone to charge density waves and a large on-site Coulombic correlation energy. In the present paper we report the solid-state characterization of a phenalenyl derivative that overcomes most of these objections and leads to unique solid-state properties.

Because of the considerations enumerated above, we felt it was important to attempt to design a molecule that avoided the problems associated with an exactly half-filled band and also circumvented the 1-dimensionality that is associated with many planar conjugated π-systems. The molecular class of choice (spiro-biphenalenyls) is exemplified below (**1**), although it should be noted that the neutral radicals derived from these compounds are still free to undergo σ-dimerization (see refs 8 and 9) at a number of positions in the phenalenyl ring.

Spiro-Biphenalenyls. We have previously reported the synthesis and solution properties of 9-oxidophenalenone complexes of boron and beryllium containing two phenalenyl units in the same molecule that are oriented at 90° to one another by virtue of the spiro-linkage.[10]

There is considerable charge separation in these molecules, as pictured in the right-most structure for the boron compound (eq 1).

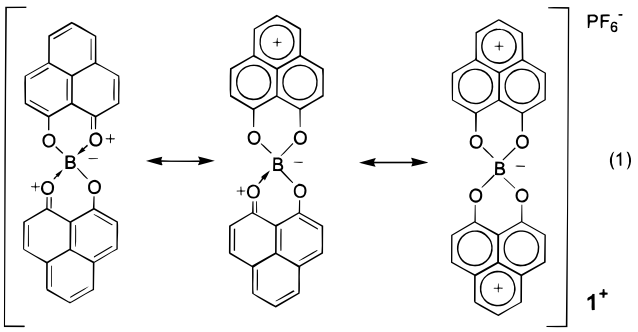

One piece of evidence that supports the idea that the 9-oxido-

[†] University of Kentucky.
[‡] University of Arkansas.
[§] University of Waterloo.

(1) Haddon, R. C. *Nature* **1975**, *256*, 394.
(2) Haddon, R. C. *Aust. J. Chem* **1975**, *28*, 2343.
(3) Haddon, R. C.; Wudl, F.; Kaplan, M. L.; Marshall, J. H.; Cais, R. E.; Bramwell, F. B. *J. Am. Chem. Soc.* **1978**, *100*, 7629.
(4) Haddon, R. C.; Chichester, S. V.; Stein, S. M.; Marshall, J. H.; Mujsce, A. M. *J. Org. Chem.* **1987**, *52*, 711.
(5) Goto, K.; Kubo, T.; Yamamoto, K.; Nakasuji, K.; Sato, K.; Shiomi, D.; Takui, T.; Kubota, M.; Kobayashi, T.; Yakusi, K.; Ouyang, J. *J. Am. Chem. Soc.* **1999**, *121*, 1619−1620.
(6) Oakley, R. T. *Can. J. Chem.* **1993**, *71*, 1775−1784.
(7) Cordes, A. W.; Haddon, R. C.; Oakley, R. T. *Adv. Mater.* **1994**, *6*, 798−802.
(8) Griller, D.; Ingold, K. U. *Acc. Chem. Res.* **1976**, *9*, 13−19.
(9) McBride, J. M. *Tetrahedron* **1974**, *30*, 2009−2022.
(10) Haddon, R. C.; Chichester, S. V.; Marshall, J. H. *Tetrahedron* **1986**, *42*, 6293.

10.1021/ja992040c CCC: $18.00
Published on Web 10/14/1999

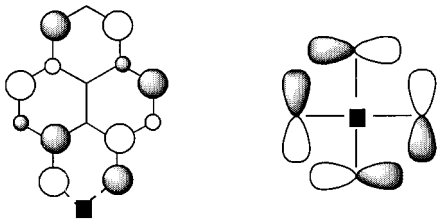

Figure 1. Spiroconjugative interaction between the phenalenyl LUMOs in **1** and **3**. As a result the LUMO (shown) and LUMO-1 of **1** and **3** consist of the symmetric and antisymmetric combinations, respectively.

phenalenone unit bears most of the positive charge comes from the electrochemistry (eq 2).

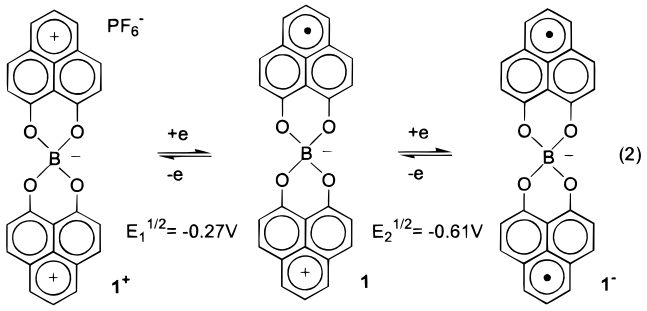

The first reduction potential of the related 1,9-diethoxyphenalenylium tetrafluoroborate ($\mathbf{2}^+$ BF_4^-) occurs at almost the same potential as that required for the reduction of $\mathbf{1}^+$ PF_6^-.

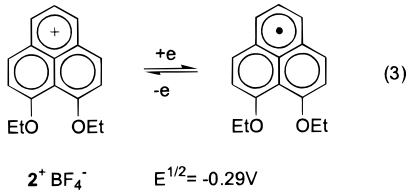

There are a number of interesting features regarding the reduced forms of $\mathbf{1}^+$ PF_6^-. ESR spectroscopy shows that the first reduction product **1** is paramagnetic as expected, but with the spin density distributed over the whole molecule so that on the time scale of the experiment the electron interacts with all of the nucleii in the molecule. However, the second reduction product $\mathbf{1}^-$, is found to be ESR silent and is therefore diamagnetic. These observations, together with the splitting seen in the first and second redox potentials of $\mathbf{1}^+$ PF_6^-, suggest that the two 9-oxidophenalenone units do not act independently but are quite strongly coupled insofar as the lowest unoccupied molecular orbital (LUMO) is concerned.

The 9-oxidophenalenone LUMO is shown in Figure 1, where the position of the spiro-junction is denoted with a solid square. Clearly the LUMOs on the two sides of the molecule are ideally positioned for a spiro-conjugative interaction, and this apparently explains the observation that the LUMO is in fact distributed over the whole of the molecule, rather than consisting of two degenerate isolated halves of the molecule.[10]

Thus, the neutral radical **1** potentially obviates most (but not all), of the objections enumerated above. First, it leads to a quarter-filled band in the solid state, and second, it must give at least a two-dimensional electronic structure provided that there is interaction between the molecules in the lattice without σ-dimerization. Thus, the question of σ-dimerization is the only variable that the present strategy does not directly address.

Results and Discussion

Preparation and Solution Properties of Radical (3). In the present paper we focus on an amino derivative, because this compound was the first to give rise to high-quality crystals of the radical that were suitable for complete solid-state characterization. We began by preparing the hexylamino variant ($\mathbf{3}^+$) of compound $\mathbf{1}^+$ via the chloride ($\mathbf{3}^+$ Cl^-), but finally employing the tetraphenylborate anion to obtain the required solubility properties for the salt. The compound $\mathbf{3}^+$ BPh_4^- gave air-stable, but highly light-sensitive yellow crystals, that could be purified by recrystallization to give material suitable for radical preparation and crystal growth.

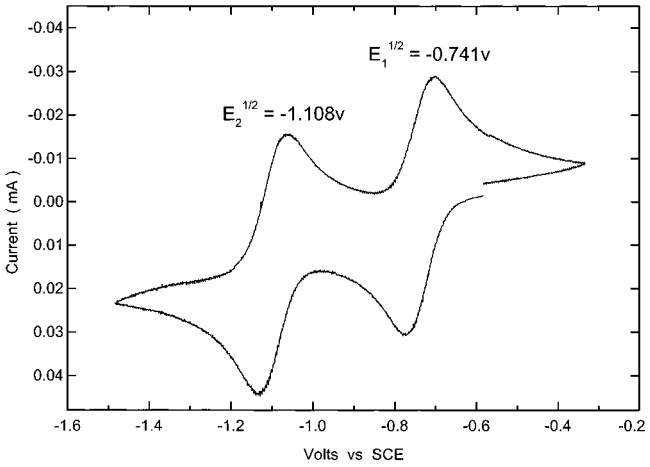

Figure 2. Cyclic voltammetry of **3** in acetonitrile, referenced to SCE via internal ferrocene (not shown).

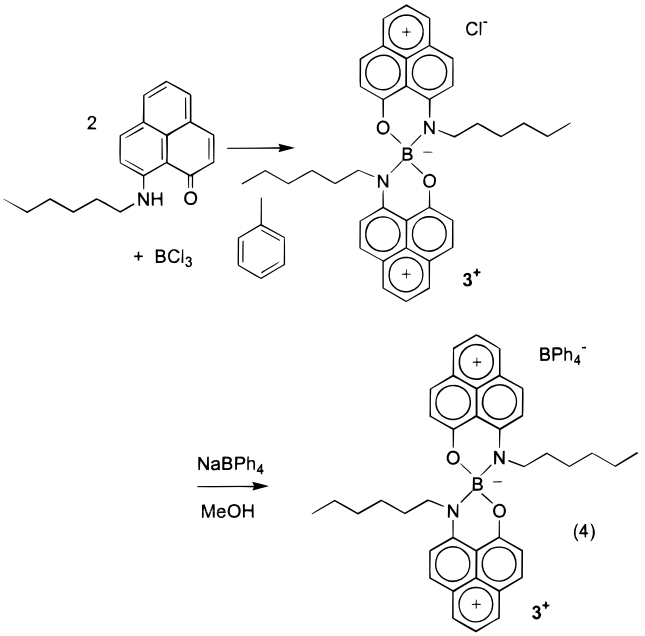

The electrochemistry of $\mathbf{3}^+$ BPh_4^- is presented in Figure 2, and it may be seen that the compound shows a well-behaved double reduction at a more negative potential than is required for $\mathbf{1}^+$ PF_6^-. As with the oxygen compound, the disproportionation potential of $\Delta E^{2-1} = E_2^{1/2} - E_1^{1/2} = -0.37$ v, is quite low. The ΔE^{2-1} value largely determines the on-site Coulombic correlation energy (U) in the solid state, and is well established as an important discriminator for organic metals.[11,12]

After a number of attempts to crystallize **3** we found that the use of a chemical reductant in an H-cell gave reproducible yields (~50%), of high quality, black lustrous, long blades of the

(11) Garito, A. F.; Heeger, A. J. *Acc. Chem. Res.* **1974**, *7*, 232−240.
(12) Torrance, J. B. *Acc. Chem. Res.* **1979**, *12*, 79−86.

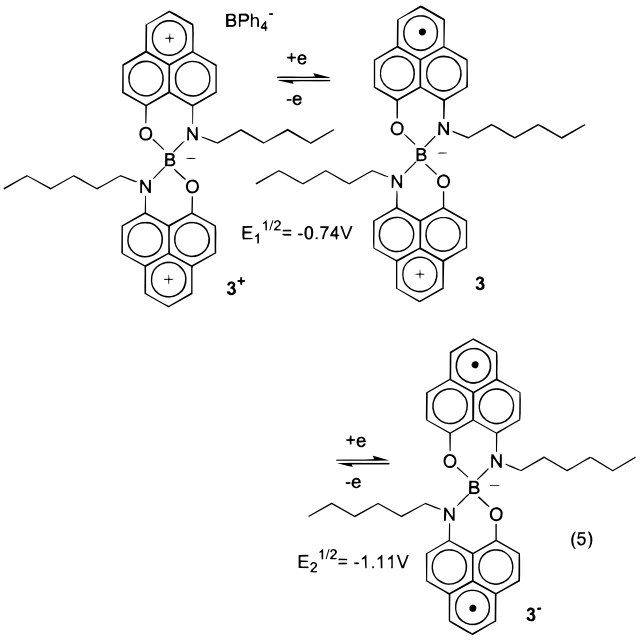

radical. We used cobaltocene as reductant because the oxidation potential ($E^{1/2} = -0.91$v),[13] falls between the $E_1^{1/2}$ and $E_2^{1/2}$ reduction potentials of $\mathbf{3}^+$ BPh_4^-. For optimum crystal quality the H-cell must be loaded in a drybox and the solvent (acetonitrile) then rigorously degassed on a vacuum line before allowing the reagents to mix. Diffusion of the solutions through the intervening glass frit gave rise to immediate crystal nucleation and the crystals reached their optimum size and quality in about one week.

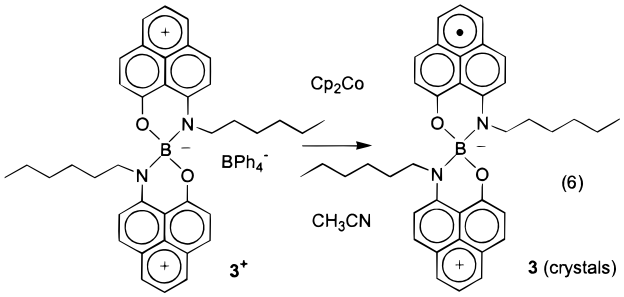

Solutions of the radical **3** are extremely oxygen-sensitive, but the crystals were quite stable to the atmosphere, and we were able to obtain chemical analyses, the X-ray crystal structure, and other solid-state measurements after handling the crystals in the air.

X-ray Crystal Structure of 3. There are eight molecules of **3** in the unit cell (four pairs of enantiomers). The most important point for our purposes is the absence of σ-dimerization. As noted above, we did not employ bulky substituents at the active positions of the phenalenyl nucleus[3,4] to suppress the type of intermolecular carbon−carbon bond formation exemplified below in eq 7.

The importance of the fact that the compound crystallizes in the form of **3** rather than **4** cannot be overemphasized. This observation demonstrates the viability of the proposal to construct an intrinsic molecular metal based on phenalenyl. It has become dogma in the field of carbon-based free radicals that steric hindrance is required to suppress the type of

(13) Robbins, J. L.; Edelstein, L.; Spencer, B.; Smart, J. C. *J. Am. Chem. Soc.* **1982**, *104*, 1882−1893.

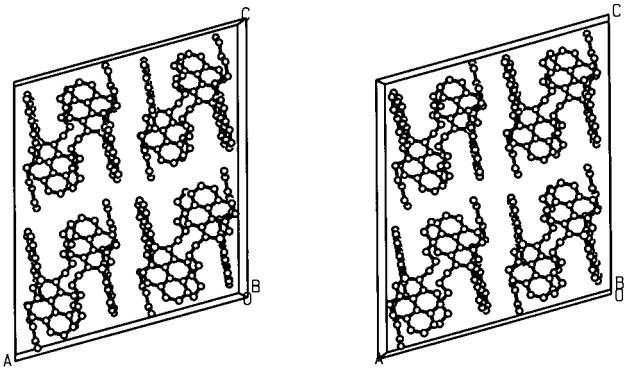

Figure 3. Steroview of crystalline **3** viewed down the *y*-axis.

σ-dimerization shown in eq 7.[14] Clearly, however, the resonance present in **3** is sufficient to stabilize the radical over the diamagnetic dimer **4**.

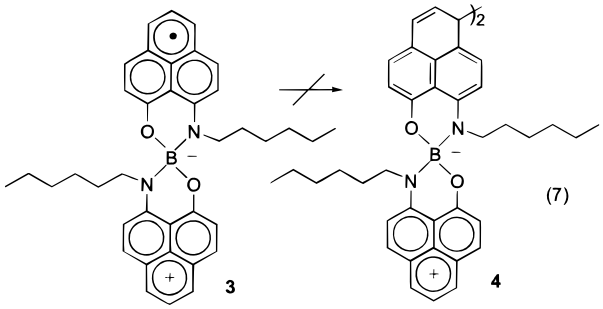

There are no inter-radical distances that are shorter than van der Waals contacts. The packing involves rows of radicals along the *x* direction which interlock with hexyl chains facing phenalenyl groups, as shown in stereo in Figure 3. The shortest distances between the spin-bearing phenalenyl units are given in Table 1, and illustrated in parts A and B of Figure 4. The intermolecular spacing is of similar distance in all three axial directions of the lattice, although the contacts are slightly shorter in the *y* (needle) direction.

Thus, for all intents and purposes, the structure of crystalline **3** resembles that of an ordinary (diamagnetic), organic molecular crystal. There are no intermolecular contacts that are closer than the normal van der Waals separation (3.4 Å for C···C), and it appears that the molecules sit in the lattice, completely independent of one another.

Magnetic Susceptibility of 3. We measured the magnetic susceptibility (χ), of **3** between temperatures (T) of 4 and 400 K, using a Faraday balance. The compound shows classical Curie magnetic susceptibility with an antiferromagnetic coupling at low temperatures (Figure 5a). By fitting the experimental data to the Curie function, we obtain a measured sample diamagnetism of $\chi_o = -380 \times 10^{-6}$ emu/mol (calculated: -365×10^{-6} emu/mol), and a Curie−Weiss constant of $\theta = 10$K.

In Figure 5b, we use the function $n = 8(\chi - \chi_o)(\theta + T)/3$, to obtain the number of Curie spins per molecule (n) as a function of temperature (T). The plot shows that in the solid state **3** behaves as a free radical with exactly one spin per molecule. The only proviso to this statement occurs at low temperatures, where the spins couple antiferromagnetically at 10 K. This ordering temperature apparently sets the energy scale (0.001 eV) for interactions between the electrons in the lattice. This very small value is supported by the X-ray crystal structure of **3**, which showed no evidence of intermolecular interactions in the lattice.

(14) March, J. *Advanced Organic Chemistry*; Wiley: New York, 1985.

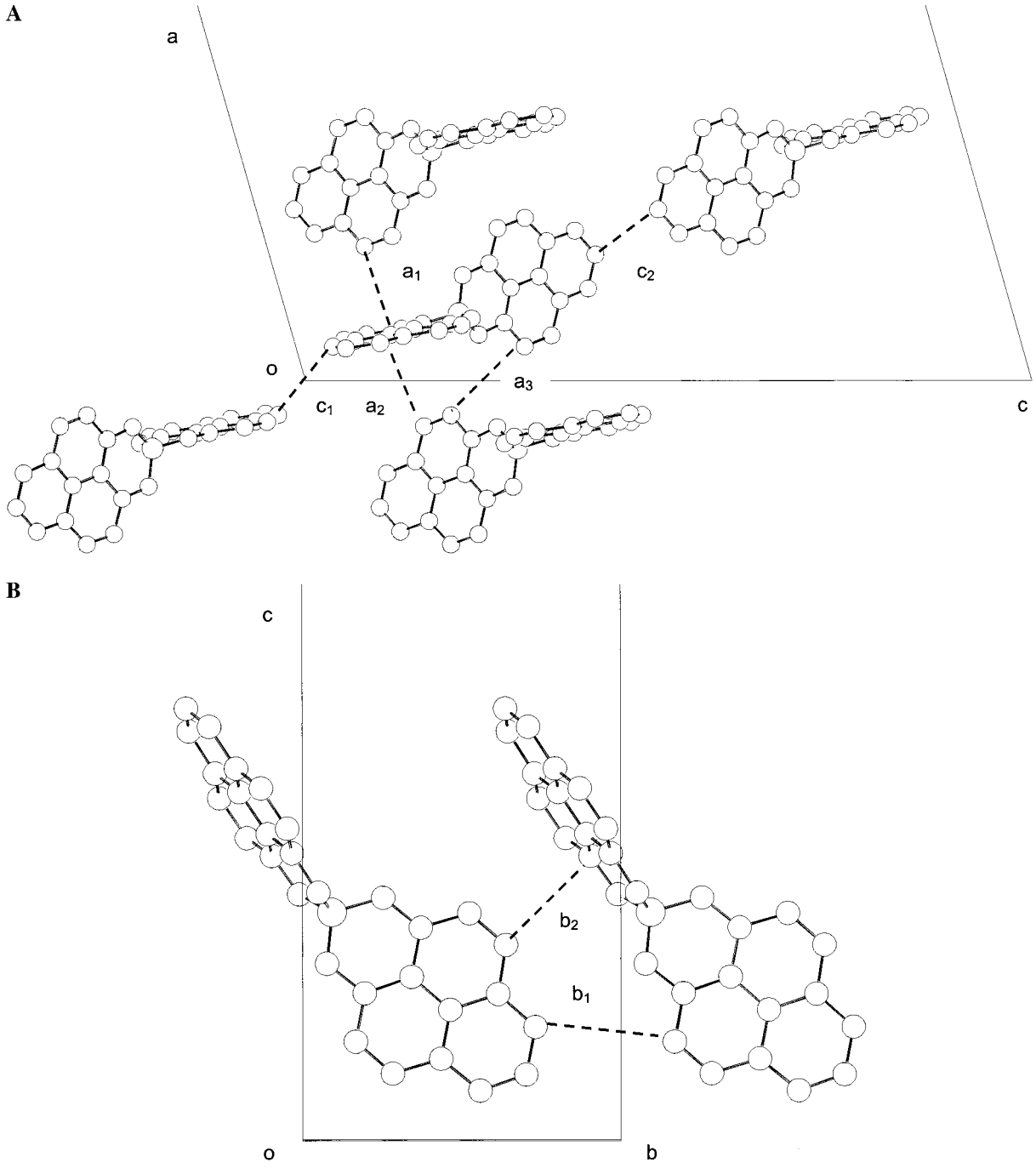

Figure 4. Closest intermolecular contacts between phenalenyl units in the crystal lattice of **3**.

Table 1. Inter-Radical C···C Contacts in Crystalline **3**

principal direction	figure label	relationship of radicals	dihedral angles (deg) between ring perpendiculars	C···C distance (Å)
a	a1	$^1/_2 - x, y + ^1/_2, ^1/_2 - z$	76.9	3.72
	a2	$-x, y + 1, ^1/_2 - z$	76.9	3.69
	a3	$-x, y, ^1/_2 - z$	72.2	3.94
b	b1	$x, y - 1, z$	0.0	3.95
	b2	$x, 1 + y, z$	84.7	3.49
c	c1	$-x, 1 - y, -z$	0.0	3.60
	c2	$^1/_2 - x, -y - ^1/_2, 1 - z$	0.0	3.63

Electrical Resistivity of 3. The electrical resistivity (ρ) of about five crystals of **3** were measured using four-probe inline contacts employing a variety of methods to make the contacts along the long axis of the blades (*b*-axis of the unit cell). A number of crystals were evaluated over the full temperature range from 60 to 375 K with identical results.

The conductivity increases with temperature but saturates above 200 K to give a room-temperature conductivity of $\sigma = 0.05$ S/cm. It is possible to fit the low-temperature data (Figure 6) to an exponential, extract an activation energy, $E_a = 0.13$ eV, and infer an energy gap, E_g(transport) $= 2\Delta = 0.26$ eV.

Band Electronic Structure of 3. The conductivity measured for crystals of **3** is the highest yet seen for a neutral radical molecular conductor[15] (see also ref 16) and is very difficult to reconcile with the solid-state packing and the measured mag-

(15) Barclay, T. M.; Cordes, A. W.; Haddon, R. C.; Itkis, M. E.; Oakley, R. T.; Reed, R. W.; Zhang, H. *J. Am. Chem. Soc.* **1999**, *121*, 969−976.

(16) Imaeda, K.; Yamashita, Y.; Li, Y.; Mori, T.; Takehiko, M.; Inokuchi, H.; Sano, M. *J. Mater. Chem.* **1992**, *2*, 115−118.

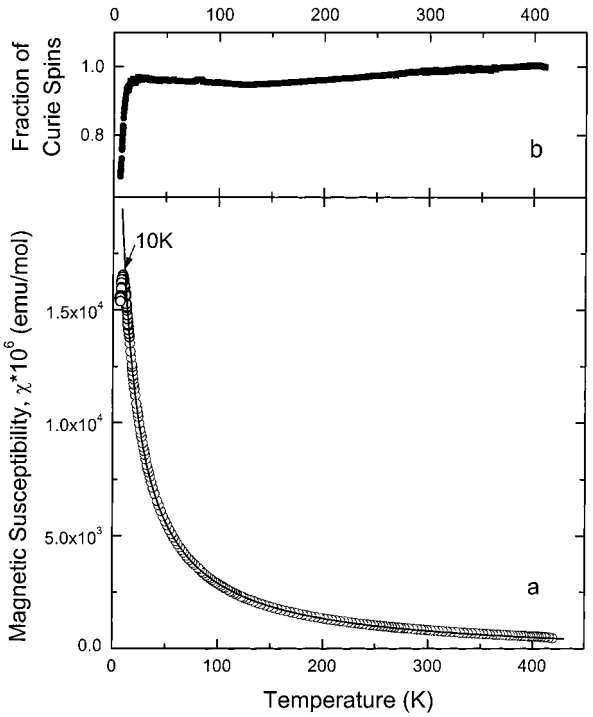

Figure 5. Magnetic susceptibility of crystalline **3** as a function of temperature together with the fraction of Curie spins per molecule (see text). The solid line is a Curie fit to the data between 20 and 300 K.

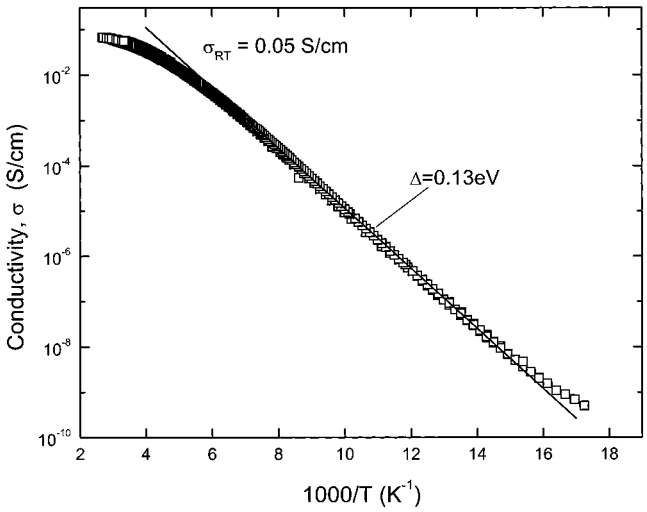

Figure 6. Single-crystal conductivity of **3** as function of temperature, measured along the needle (b and b*) axis.

netic susceptibility which provide no evidence for a conducting pathway in the lattice.

In an effort to address this question, we carried out extended Huckel theory (EHT) band structure calculations[17] on the crystal structure. Such calculations have been very useful in understanding the electronic structure of the organic molecular superconductors[18] and thin-film field effect transistors[19] but cannot be expected to succeed in situations where the tight-binding approximation is not applicable.

The results are shown in Figure 7 for the calculation carried out on the lattice found in the X-ray crystal structure, whereas

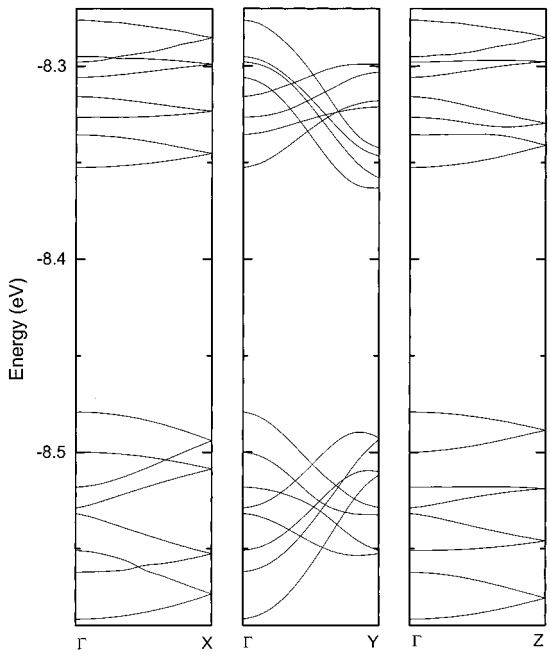

Figure 7. EHT band structure calculated for the experimental structure of crystalline **3**.

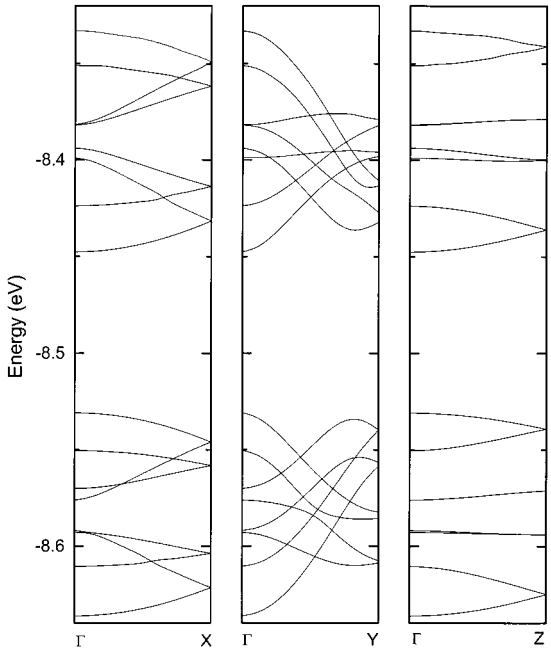

Figure 8. EHT band structure calculated for the experimental structure of crystalline **3**, but with the hexyl group replaced with hydrogen.

in Figure 8 the calculation is carried out with the hexyl group replaced by a hydrogen substituent on the nitrogen.

The 16 bands shown in the figures are derived from the two LUMOs of $\mathbf{3}^{+}$, for each of the eight molecules of **3** in the unit cell; these basically consist of the symmetric and antisymmetric combinations of the LUMO shown in Figure 1 (see also ref 10). Alternatively, they can be viewed as arising from the nonbonding molecular orbitals[1,2] of each of the 16 phenalenyl units in the unit cell. In a band picture these 16 orbitals now accommodate a total of eight electrons, leading to a quarter-filled band. The tight binding picture fails of course, because the magnetic susceptibility shows that the electrons are unpaired in this compound over the whole temperature range. The organic molecular superconductors, show a temperature independent

(17) Hofmann, R. *Solids and Surfaces*; VCH: New York, 1988.
(18) Haddon, R. C.; Ramirez, A. P.; Glarum, S. H. *Adv. Materials* **1994**, *6*, 316−322.
(19) Haddon, R. C.; Siegrist, T.; Fleming, R. M.; Bridenbaugh, P. M.; Laudise, R. A. *J. Mater. Chem.* **1995**, *5*, 1719−1724.

Pauli magnetic susceptibility over the full range of temperatures, with values of $\chi_P \approx (100-1500) \times 10^{-6}$ emu/mol. EHT calculations give a value of about 0.5 eV for the bandwidths (W), of most of the organic molecular superconductors. The tight-binding approximation holds quite well for these materials, and Fermi surface properties can be qualitatively interpreted by EHT band theory. Nevertheless, the magnetic susceptibilities are enhanced by a factor of 2−3 over those predicted by density of states estimates based on the EHT band calculations, presumably as a result of the strong correlations present in these systems (large on site Coulombic correlation energy, U).[18] Thus, to a first approximation, it seems that crystalline **3** must be considered as a degenerate Mott−Hubbard insulator, in the narrow band limit, albeit with a small value of U.

The total dispersion in the band structure for all of these orbitals is 0.31 eV; however, most of this spread in energy levels comes through the intramolecular spiro-interaction between the phenalenyl units that splits the energy bands into two subgroups of eight levels. An EHT calculation carried out on a single molecule of **3** (using the experimental molecular structure), placed these energy levels at −8.55 and −8.35 eV, for a splitting of 0.20 eV for the spiroconjugative interaction. The point of maximum subgroup dispersion occurs at Γ(0.11 eV), but inspection of the band structure shows that the single bands of maximum dispersion are 0.024 eV (along a^*), 0.075 eV (b^*), 0.014 eV (c^*). In a tight-binding picture the electrons would half-fill the lower subgroup of energy bands, but this model is not supported by the magnetic data, and as a first approximation we consider the electronic structure of **3** within a hopping picture. The most straightforward interpretation would then assign the energy gap observed in the conductivity, $E_g = 0.26$ eV, as arising from the on-site Coulombic correlation energy (U); previously estimated in solution from the electrochemistry of **3** as $\Delta E^{2-1} = 0.37$ v.

If we assume that all of the unpaired electrons (n) in the lattice of **3** contribute to the conductivity, then we can obtain the mobility (μ) of the carriers from the relationship $\sigma = ne\mu$, where σ is the conductivity and e is the electronic charge. In this way we estimate the room-temperature mobility of the carriers in **3** as $\mu = 2.6 \times 10^{-4}$ cm^2/Vs. Mobilities of the organic molecular superconductors generally have values of $\mu \approx 1$ cm^2/Vs;[20] however, the number of carriers is frequently less than that estimated from a simple count based on the valence of the organic molecule. Field-effect mobilities for transistors based on organic semiconductors are in the range, $\mu \approx 1-10^{-4}$ cm^2/Vs, but in general the bandwidths from EHT theory for the organic semiconductors and superconductors are about $W \approx 0.2-0.5$ eV.[18,19,21]

In an effort to further analyze the conduction mechanism in **3** we repeated the band-structure calculations with all of the hexyl groups replaced by hydrogen. As may be seen in Figures 7 and 8, the main change is a reduction in the energy gap between the two band subgroups. With the hexyl group (experimental structure), the energy gap is 0.127 eV, whereas in the absence of the hexyl group the energy gap between subgroups falls to 0.083 eV. The effects on the other features are quite minor; the bandwidth of the lower subgroup changes from 0.108 eV to 0.106 eV, whereas the bandwidth of the upper subgroup changes from 0.077 to 0.115 eV when the hexyl group is removed from the calculation. On the basis of these calculations it seems that the only function of the hexyl group is steric repulsion with the conjugated part of the molecule, although it is possible that the hexyl group is involved in the conduction pathway in a manner that is not captured by the EHT calculations.

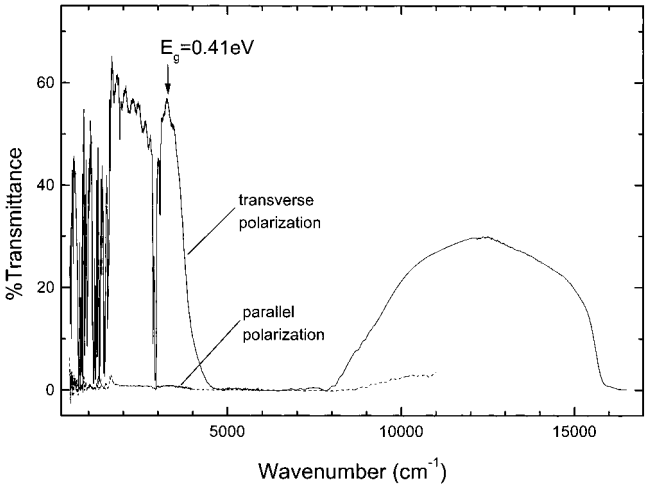

Figure 9. Single-crystal IR and UV−visible transmission spectrum of crystalline **3** (resolution of 4 cm^{-1}).

Electronic Excitations in Solid State 3. We decided to seek further information on the electronic structure by measuring the electronic excitations in crystals of **3**. This was possible because of the bladelike morphology of the crystals, some of which are quite thin. We chose a crystal for mounting in our spectrometer that had dimensions of 2.5 mm (parallel direction, b-axis of the unit cell, b^*-axis of the reciprocal unit cell and also the axis along which the resistivity was measured) × 100 μm (transverse direction, approximately along the vector from −4,0,1 to 4,0,−1) × 10 μm (direction of incident light beam, perpendicular to the flat face of the blade, along the c^*-axis of the unit cell).

The results are presented in Figure 9 where we show the transmittance (T) through the crystal with light polarized in the transverse and perpendicular directions. As may be seen, we find an optical energy gap, E_g(optical) ≈ 0.5 eV (∼4000 cm^{-1}), and a total bandwidth (valence + energy gap + conduction) of $W \approx 1.0$ eV (∼8000 cm^{-1}). All of these excitations occur in the near-infrared (NIR) region, and measurements in the visible confirm that the material is transparent in the region 1−2 eV, accounting for the red color of very thin crystals in transmission. There is a significant anisotropy in the spectra taken with different polarizations. The transmittance (T) in the gap in the transverse direction is 0.4, whereas it is 0.015 in the parallel direction. Thus, using the relationship $T = (1 - R)^2 \exp(-\alpha d)$, where R is the reflectance, α is the absorption coefficient, and d is the thickness, we estimate R(transverse) = 0.37, and R(parallel) = 0.88. The absorptions in the mid-IR, between 450 and 3100 cm^{-1}, are due to the molecular vibrations of the radical **3**.

These measurements present a further dilemma to our attempts to interpret the electronic structure of crystalline **3**, in that the excitation spectra show evidence of a well-developed band of total width, $W = 1.0$ eV, conduction bandwidth, W(CB) = 0.5 eV, and energy gap, E_g(optical) = 0.5 eV. Furthermore, the anisotropy seen in the optical spectrum also argues for well-developed energy bands in crystalline **3**, particularly along b^*. Taken at face value, these results suggest that the band-structure calculations have underestimated the conduction bandwidth and energy gap by a factor of at least 3, which is extremely difficult

(20) Murata, K.; Ishibashi, M.; Honda, Y.; Fortune, N. A.; Tokumoto, M.; Kinoshita, N.; Anzai, H. *Solid State Commun.* **1990**, *76*, 377−381.

(21) Schon, J. H.; Kloc, C.; Laudise, R. A.; Batlogg, B. *Phys. Rev. B* **1998**, *58*, 12952−12957.

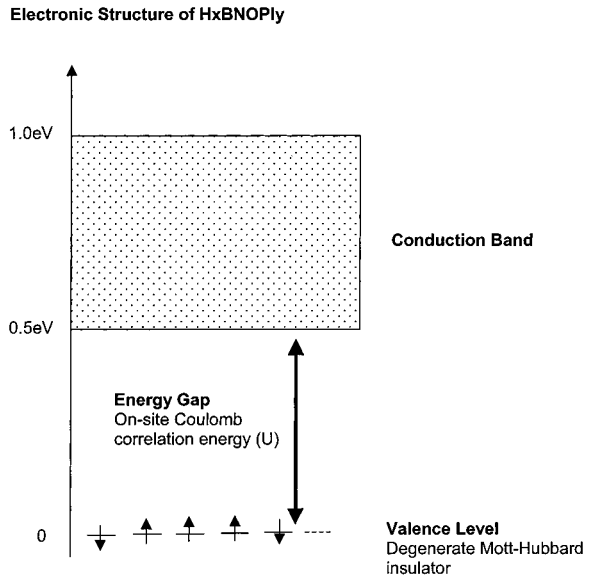

Figure 10. Proposed electronic structure of crystalline **3**.

to rationalize with the crystal structure and the magnetic susceptibility.

We therefore consider a modification to the hopping model given above. We propose that the ground state of crystalline **3** does indeed correspond to that of a degenerate Mott−Hubbard insulator but that this localized ground state lies below the delocalized electronic states seen in the band structure calculations by *U*, the on-site Coulombic correlation energy (Figure 10). On the basis of the optical spectrum and the electrochemistry, we estimate $U \approx 0.4$ eV in crystalline **3**. The width of the conduction band (0.5 eV) then encompasses all 16 of the energy levels shown in Figure 7 and is apparently underestimated by a factor of 2 in the band-structure calculations.

We now adapt this model to a treatment of mobility that has been used to account for charge transport in a variety of molecular conductors.[22] In the mobility model,[22] the number of carriers (n_c) and the mobility are both temperature-dependent, and thus the conductivity is given by $\sigma(T) = n_c(T)e\mu(T)$, where $n_c(T) = n \exp(\Delta/kT)$ and $\mu(T) = AT^{-\alpha}$. A fit of this function to our data gives $\alpha = 5.5$, $E_g = 2\Delta = 0.4$ eV, $\mu(T = 300\ \text{K}) = 0.4\ \text{cm}^2/\text{V s}$ and $\mu(T = 100\ \text{K}) = 170\ \text{cm}^2/\text{V s}$. The strong temperature dependence in the mobility originates from the scattering by optical phonons (molecular vibrations). In our adaptation of this model the relevant energy gap (Δ), is simply given by $\Delta = U$, the on-site Coulombic correlation energy. Thus, the transport properties of crystalline **3** arise from thermal population of the energy bands given in Figure 7 which together comprise the conduction band. The ground state is localized and thus leads to Curie behavior in the measured magnetic susceptibility.

Conclusion and Summary

The properties of crystalline **3** challenge some current dogmas: (1) that carbon-based radicals are only monomeric as the result of steric hindrance, (2) that charge-transfer salts are the only route to molecular conductors, (3) that stacking is necessary for conductivity in molecular conductors, (4) that strong intermolecular orbital overlap is necessary for the development of delocalized energy bands and band transport in organic solids, (5) that magnetism, resistivity, structure, and band structure are well-correlated in organic solids.

Most important, however, is the promise offered by this new class of molecular conductors. The crystallization of **3**, and the properties reported herein, clearly establish the merits of the neutral radical approach to organic molecular conductors. A large range of derivatives is available, and if they can be crystallized (without σ-dimerization), it should be possible to increase the bandwidths and so obtain intrinsic molecular metals and superconductors.

Experimental Section

Materials. Boron trichloride (Aldrich), sodium tetraphenylborate (Aldrich) and cobaltocene (Strem) were all commercial products and were used as received. 9-*N*-Hexylamino-1-oxo-phenalene was synthesized according to literature procedures.[23] Toluene was distilled from sodium benzophenone ketyl just prior to use. Acetonitrile was distilled from P_2O_5 immediately before use.

Preparation of 3^+, Cl^-. 9-*N*-Hexylamino-1-oxo-phenalene (1.4 g, 0.005 mol) in toluene (100 mL) was treated with boron trichloride in dichloromethane (2.5 mL, 0.0025 mol) under argon in the dark, and the mixture was refluxed overnight. The yellow solid was isolated by filtration (0.6 g, 40%). IR (ATR, 4000−680 cm^{-1}): 2954 (m), 2927 (m), 2856 (m), 1629 (m), 1573 (m), 1588 (s), 1518 (m), 1486 (vw), 1470 (w), 1449 (m), 1414 (w), 1392 (m), 1358 (m), 1336 (w), 1297 (s), 1244 (m), 1192 (m), 1175 (w), 1134 (m), 1102 (w), 1048 (m), 1017 (s), 1001 (w), 976 (w), 904 (w), 883 (w), 856 (m), 847 (m), 825 (w), 789 (w), 767 (w), 728 (w), 707 (w).

Preparation of 3^+, BPh_4^-. A solution of 0.5 g of Na BPh_4 in 20 mL of MeOH was carefully added to a solution of 3^+, Cl^-, (0.6 g) in 40 mL of MeOH. The solution immediately became cloudy. After several hours, small red crystals formed on the bottom of the flask. After filtration, 0.46 g of red crystals were obtained and stored in the dark. The crystals were purified by recrystallization from a dichloromethane/methanol mixture. ^{1}H NMR (CD_3CN): δ 8.52 (d, 2H), 8.43 (d, 2H), 8.32 (m, 4H), 7.81 (t, 2H), 7.45 (m, 4H), 7.26 (b, 8H), 6.98 (t, 8H), 6.83 (t, 4H), 3.64 (b, 2H), 3.27 (b, 2H), 1.73 (b, 4H), 1.13 (vb, 12H), 0.59(t, 6H). IR (4000−400 cm^{-1}): ν = 3056 (m), 3033 (m), 2955 (m) 2926 (m), 2855 (m), 1951 (w), 1628 (s), 1585 (s), 1573 (s), 1585 (s), 1515 (s), 1470 (m), 1446 (m), 1425 (w), 1413 (w), 1389 (m), 1357 (m), 1333 (w), 1294 (s), 1244 (m), 1190 (m), 1166 (m), 1136 (m), 1100 (w), 1040 (m), 1016 (m), 963 (w), 903 (w), 879 (w), 845 (m), 824 (w), 769 (w), 731 (m), 706 (m), 612 (w), 580 (w), 549 (w), 494 (w). Anal. Calcd for $C_{62}H_{60}O_2N_2B_2$: C, 83.97; H, 6.82; N, 3.16; B, 2.44. Found: C, 84.38; H, 6.75; N, 3.40; B, 2.31.

Crystallization of 3. An invertable H-Cell with a glass D frit was loaded in a drybox. A solution of 150 mg of 3^+, BPh_4^- in 20 mL of dry CH_3CN was placed in one container, and 40 mg Cp_2Co was dissolved in 20 mL of dry CH_3CN in the other container. The containers were attached to the inverted H-cell. The H-cell was removed from the drybox and attached to a vacuum line, and the containers were taken through three cycles of freeze, pump, and thaw to degas the solutions. The H-cell was inverted, and the solutions allowed to diffuse through the glass frit. After sitting in the dark for one week the cell yielded 60 mg of black shining blades. IR (ATR, 4000−680 cm^{-1}): 2954 (m), 2927 (m), 2855 (m), 1626 (m), 1586 (w), 1565 (s), 1536 (w), 1510 (m), 1487 (vw), 1465 (m), 1442 (m), 1414 (vw), 1389 (w), 1350 (m), 1331 (m), 1287 (s), 1238 (s), 1191 (m), 1156 (m), 1136 (m), 1112 (w), 1099 (w), 1065 (m), 1056 (m), 1037 (m), 1008 (m), 990 (s), 965 (m), 935 (m), 910 (w), 879 (m), 848 (m), 831 (m), 811 (w), 789 (vw), 771 (m), 760 (m), 754 (m), 723 (w), 716 (w), 695 (m), 682(m). Anal. Calcd for $C_{38}H_{40}O_2N_2B$: C, 80.42; H, 7.10; N, 4.94; B, 1.90. Found: C, 79.92; H, 7.02; N, 5.15; B, 1.81.

X-ray Crystallography. Data were collected on a Nonius KappaCCD diffractometer at 173 K. The black crystal gave a monoclinic unit cell (space group *C*2/*c*, $Z = 8$), with unit cell parameters a = 24.330(2) Å, b = 8.926(1) Å, c = 28.394(2) Å, β = 105.93(1)°, and V = 5929.5(9) A^3. The structure was refined with 5139 reflections yielding $R = 0.089$. Full details, including bond lengths and bond angles, are given in the Supporting Information.

(22) Epstein, A. J.; Conwell, E. M.; Miller, J. S. *Ann. N. Y. Acad. Sci.* **1978**, *313*, 183−209.

(23) Haddon, R. C.; Chichester, S. V.; Mayo, S. L. *Synthesis* **1985**, 639−641.

Magnetic Susceptibility Measurements. The magnetic susceptibility was measured over the temperature range 5−420 K on a George Associates Faraday balance operating at 0.5 T.

Conductivity Measurements. The single-crystal conductivity, σ, of **3** was measured in a four-probe configuration. The in-line contacts were made with silver paint. The sample was placed on a sapphire substrate, and electrical connections between the silver paint contacts and substrate were made by thin, flexible 25 μm diameter silver wires to relieve mechanical stress during thermal cycling of the sample. The temperature dependence of the conductivity was measured in the range 373−60 K. Below 60 K the sample resistance exceeded 10^{13} Ω, the limit of the experiment. The data are presented for a crystal with dimensions $25 \times 100 \times 3000\ \mu m^3$. The same conductivity was obtained for a much thicker crystal, ruling out the influence of surface conductivity on the data.

Conductivity was measured in a custom-made helium variable-temperature probe using a Lake Shore 340 temperature controller. A Keithley 236 unit was used as a voltage source and current meter, and two 6517A Keithley electrometers were used to measure the voltage drop between the potential leads in a four-probe configuration.

Single-Crystal IR and UV−vis Transmission Spectroscopy. For the polarized IR transmission measurements a KRS-5 substrate was coated with a 2500 Å thick copper film so as to produce a long narrow slit ($60 \times 2000\ \mu m^2$). A thin single crystal of **3** with dimensions $10 \times 100 \times 2500\ \mu m^3$ was placed on the substrate so that the open slit was completely covered by the crystal. In the finished mounting, only radiation transmitted through the sample was detected (no stray light). Data were normalized on the spectra of the slit itself without the sample. For the UV−vis spectral range, the same sample mount was used with a sapphire substrate.

Three other crystals of different dimensions were measured and showed similar results. The infrared transmission measurements employed a FTIR Nicolet Magna-IR 560 ESP spectrometer. UV−vis transmission was measured with a Shimadzu UV-2501PC spectrometer.

Band-Structure Calculations. The band-structure calculations made use of a modified version of the extended Huckel theory (EHT) band-structure program supplied by M.-H. Whangbo. The parameter set is chosen to provide a reasonably consistent picture of bonding in heterocyclic organic compounds.[19,24]

Acknowledgment. This work was supported by the Office of Basic Energy Sciences, Department of Energy under Grant No. DE-FG02-97ER45668.

Supporting Information Available: Tables of crystallographic and structural refinement data, atomic coordinates, bond lengths and angles, and anisotropic thermal parameters (PDF). This information is available free of charge via the Internet at http://pubs.acs.org.

JA992040C

(24) Cordes, A. W.; Haddon, R. C.; Oakley, R. T.; Schneemeyer, L. F.; Waszczak, J. V.; Young, K. M.; Zimmerman, N. M. *J. Am. Chem. Soc.* **1991**, *113*, 582.